

Traveling-wave atom–cavity interaction in the single-atom microlaser

K. An, R. R. Dasari, and M. S. Feld

George R. Harrison Spectroscopy Laboratory, Massachusetts Institute of Technology, Cambridge, Massachusetts 02139

Received May 30, 1997

We demonstrated traveling-wave atom–cavity interaction in the single-atom microlaser by tilting the atomic beam from its usual orientation of normal incidence with respect to the cavity mode. Laser-tuning curves, measured for various excitation pulse areas, are in good agreement with one-atom microlaser–maser theory. © 1997 Optical Society of America

In recent years the simple physical system composed of a single atom strongly interacting with a single mode of a cavity¹ has drawn much attention.² As one of the simplest and most fundamental forms of matter–radiation interaction, this system permits theoretical investigations from first principles. In addition, the coherent nature of the atom–cavity interaction can lead to highly nonclassical statistics of the photons confined by the cavity.^{3,4} For this reason the micromaser,⁵ which was invented more than a decade ago, still commands great theoretical interest for studies such as generation of nonclassical atom and (or) photon states or statistics.⁶ The micromaser’s optical analog, the microlaser,^{7,8} operating in the regime of nonnegligible atomic damping, is stimulating similar interest among both experimentalists and theorists^{9,10} and has the potential to serve as a gateway to practical applications.

In the microlaser,⁷ two-level atoms in a beam, which are excited by a π -pulse excitation field before entering a resonator, traverse the resonator one by one. Inside the resonator each atom can emit a photon by the quantized atom–cavity Rabi interaction. Usual spontaneous emission is negligible for atoms with the most-probable velocity during their transit through the resonator. The ultrahigh Q of the resonator (2×10^9) permits substantial photon storage, so that in the steady state several photons, on average, can be maintained inside the resonator, even when the average number of atoms in the resonator is of the order of unity.

In the above experiment the atomic beam intersects the cavity axis at a right angle, and the atoms can interact simultaneously with both traveling-wave components of the standing-wave cavity mode. However, the standing-wave nature of this mode, which arises naturally in a Fabry–Perot resonator, significantly limits nonclassical features of the coherent atom–cavity interaction. This limit comes about because the standing-wave cavity mode varies periodically in space on the scale of an optical wavelength. The atomic beam, by which atoms are injected into the cavity, is much larger than a wavelength in diameter. Therefore the magnitudes of the coupling constants of atoms entering the microlaser cavity will vary between zero and their maximum value in a random way, de-

termined by the exact position of the atom along the cavity axis. As a result the coherent and nonclassical features of the microlaser operation are lost.⁸ It is therefore important to eliminate the position dependence of the coupling constant for different atoms to preserve the nonclassical features of single-atom laser operation, such as nonclassical photon statistics and atom–field entanglement.

One possible way of eliminating this position dependence would be to use a microscopic array of slits with a periodicity equal to the wavelength of the cavity field. When the array is properly aligned, only atoms traveling along the antinodes of the standing-wave mode would be admitted into the cavity. However, implementation of this approach poses severe technical difficulties. Another way of eliminating the position dependence would be to employ a ring resonator with an optical isolator, which would permit only one traveling-wave component to circulate. However, the optical path of this ring resonator would have to be extremely short, a few millimeters at most, to provide the conditions for a large atom–cavity coupling constant, and ultrahigh finesse ($\sim 10^6$) would be required; these two conditions are difficult to achieve simultaneously in a ring resonator.

In this Letter we introduce a simple scheme for a uniform atom–cavity coupling constant along the cavity axis and report its implementation. If the atomic beam is tilted by a small angle θ ($\ll 1$) from its usual right-angled orientation with respect to the cavity axis, the two oppositely propagating traveling-wave modes become nondegenerate with respect to the atom–cavity interaction. For an atom traveling with velocity v along the atomic beam, photons of wavelength λ emitted into the cavity in opposite directions will be Doppler shifted in frequency by $\pm v\theta/\lambda$ (in hertz) (Fig. 1). When the cavity is tuned to one of these frequencies, the interaction with the other frequency is suppressed. Note that the frequency shift is proportional to atomic velocity v . Thus, in the laboratory frame, photons emitted by atoms with different velocities will have different frequencies. Therefore, by adjusting the cavity detuning, we can select a particular velocity group of atoms in the atomic beam to interact with one of the traveling-wave modes of the cavity. Note, however, that this technique works only when

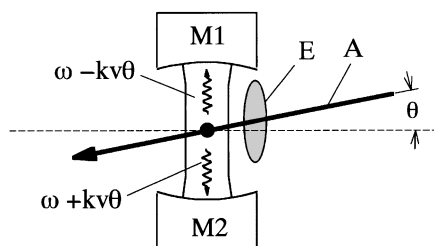


Fig. 1. Experimental setup: M1, M2, supercavity mirrors; θ , angular field tilt of the atomic beam; A, atomic beam; E, excitation field.

the frequency shift is much larger than both the cavity linewidth and the natural linewidth of the two-level transition of the atom. Otherwise, the atom would simultaneously interact with both traveling-wave components. It should also be noted that in the traveling-wave configuration coupling constant g is reduced by a factor of $\sqrt{2}$ compared with the peak standing-wave value.

An experiment was performed to demonstrate this. The setup is similar to that of Ref. 7. The resonator has a finesse of 8×10^5 with a length of 1.1 mm, so that its decay time is $\sim 1 \mu\text{s}$. The radius of curvature of the resonator mirrors is 10 cm. The waist of the resonator TEM_{00} mode is $\sim 40 \mu\text{m}$. As a result the uniform traveling-wave atom-cavity coupling constant g becomes $2\pi \times 240 \text{ kHz}$. The barium atomic beam has a diameter of $\sim 340 \mu\text{m}$, and its intersecting angle with the resonator axis can be varied (Fig. 1). The transition $^1S_0 \leftrightarrow ^3P_1$ of ^{138}Ba ($\lambda = 791 \text{ nm}$) is used for laser oscillation. Figure 2 shows the microlaser output as a function of cavity-atom detuning for various atomic-beam tilt angles. Since the transverse-mode spacing of the resonator is 6.5 GHz, much larger than the Doppler shifts that are due to the atomic-beam tilt, the coupling of the atoms to the non-resonant (transverse) modes is negligible. The mean intracavity atom number $\langle N \rangle$ is fixed well below unity, which ensures not only that the microlaser operates in the single-atom regime but also that the thresholdlike transition in the mean intracavity photon number $\langle n \rangle$,^{7,8} which occurs when $\langle n \rangle \sim 1$, is avoided. Under these conditions the laser output photocounts, which are proportional to $\langle n \rangle$, are in turn proportional to $\langle N \rangle$ for fixed cavity-atom detuning. Therefore we can regard the measured line shapes as approximate gain profiles of the single-atom microlaser. The two peaks in Fig. 2, clearly distinguished at large tilt angles, correspond to the two traveling-wave components, which are resonant at opposite cavity-atom detunings. The separation of these two peaks increases linearly with tilt angle.

Figure 3(a) shows details of such a curve for a 10-mrad tilt angle. This curve can be approximated by the convolution of the gain profile associated with an atom moving with velocity v , with velocity-distribution function $f(v)$ of the atomic beam. In the experiment the velocity-distribution function inside the resonator was independently measured. For this measurement, a probe dye laser (Coherent 599) excited the atomic beam inside the cavity at an angle of $\sim 20^\circ$ between

the atomic beam and the probe. The probe laser was scanned across the $^1S_0 \leftrightarrow ^1P_1$ transition of atomic

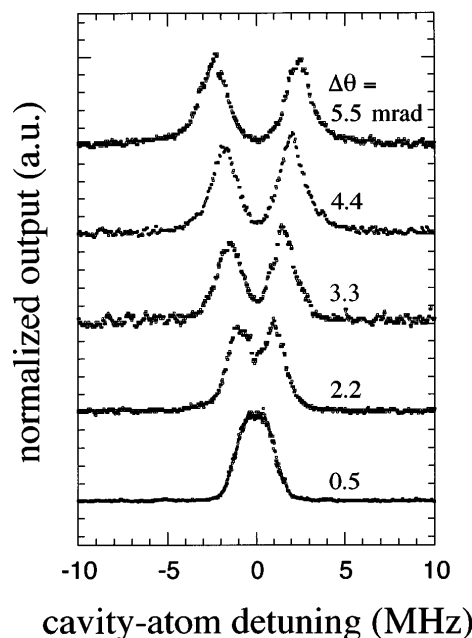


Fig. 2. Transition from standing-wave to traveling-wave interaction. Microlaser output intensity photocounts are measured as a function of cavity-atom detuning for various atomic-beam tilt angles.

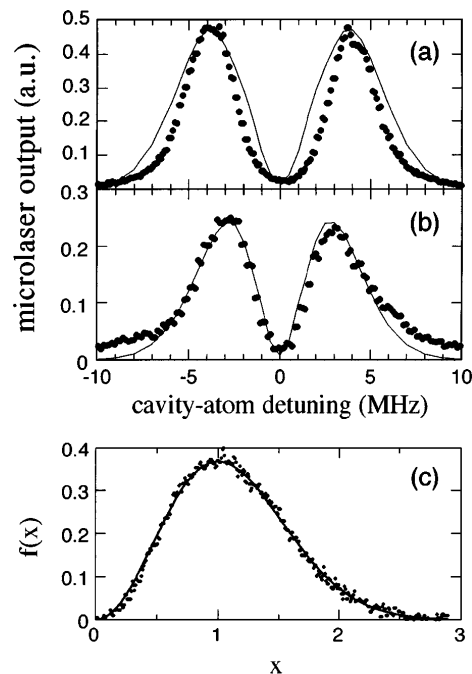


Fig. 3. Detailed plots of microlaser output versus cavity-atom detuning at a large atomic-beam tilt ($\theta \sim 10 \text{ mrad}$) with $\langle N \rangle$ fixed (≈ 0.5). (a) Pump laser optimized for the largest peak signal, which occurs when the pulse area of the excitation field is 0.7π for the mean thermal atomic velocity, (b) excitation pulse area reduced by a factor of 2 from that of (a), (c) velocity distribution of the atomic beam measured inside the cavity.

barium ($\lambda = 556$ nm), and fluorescence to the side was recorded. Since inhomogeneous broadening owing to the velocity distribution (~ 1 GHz) is much larger than the homogeneous linewidth of the transition (~ 20 MHz), the measured fluorescence line shape approximates the velocity-distribution function. This line shape is fitted by the Maxwell–Boltzmann distribution function for a beam, $f(x) = x^2 \exp(-x^2)$, with $x = v/u$, where u is the mean thermal velocity, defined as $u = (2k_B T/M)^{1/2} \sim 320$ m/s, where k_B is the Boltzmann constant, T is the oven temperature, and M is the mass of a barium atom [Fig. 3(c)].

Since the gain profile of the atom is broadened by transit-time broadening, which is proportional to the velocity of the atom, the resulting convolution curve is roughly proportional to $xf(x) \propto x^3$. To describe the measured line shape correctly, one should multiply this curve by a gain factor that accounts for the atomic polarization as well as the population inversion created by the excitation laser field. In the experiment the atoms are excited by the excitation field, which can be adjusted to a π pulse for a particular velocity group of atoms so that these atoms are completely inverted and carry no polarization. Atoms in the beam with other velocities, however, are not completely inverted. These atoms, being excited into a superposition state, attain both population inversion and polarization. For Fig. 3(a) the excitation pump is adjusted for the maximum signal size, which occurs when the pump is adjusted to a pulse area of 0.7π for the mean thermal velocity of atoms, so that both the polarization and population optimally enhance laser output. In Fig. 3(b) the pulse area of the excitation laser is reduced by half of that shown in Fig. 3(a), resulting in a different tuning curve, with the peaks occurring at smaller cavity–atom detunings.

The above convolution argument, although it is intuitive, does not provide an accurate way of incorporating the effect of the polarization and its velocity dependence into the data analysis. Instead, the fitted curves overlaid in Figs. 3(a) and 3(b) are based on the microlaser–maser theory,^{7,11} by which $\langle n \rangle$ can be calculated for a given velocity of atoms, with the Doppler shift incorporated into the cavity–atom detuning parameter. The result is then averaged over the Maxwell–Boltzmann distribution. The fits provide correct positions of the peaks, although there exist discrepancies in shape for small and large detunings.

The discrepancies at small detunings likely are due to the fact that the atomic spontaneous-emission loss, which is neglected in the above theory, becomes important for slow velocities, reducing signal size. Furthermore, since the diameter of the atomic beam is much larger than the resonator mode waist, the coupling constant is averaged over the Gaussian profile in the transverse directions. This averaging is neglected in the above analysis, likely resulting in a fitting error.

In conclusion, a scheme for realizing traveling-wave atom–cavity interaction in the microlaser has been experimentally demonstrated. It is shown that this scheme also leads to automatic velocity selectivity in the atom–cavity interaction. The present scheme should permit well-defined atom–cavity interactions in the microlaser, leading to nonclassical atom–photon statistics.⁸

This study was supported by the National Science Foundation under grants PHY-9512056 and CHE-9304251.

References

1. E. T. Jaynes and F. W. Cummings, Proc. IEEE **51**, 81 (1963).
2. S. Haroche and D. Kleppner, Phys. Today **42**(1), 24 (1989); S. Haroche and J. Raimond, Sci. Am. **268**(4), 54 (1993).
3. G. Rempe, H. Walther, and N. Klein, Phys. Rev. Lett. **58**, 353 (1987).
4. M. G. Raizen, R. J. Thompson, R. J. Brecha, H. J. Kimble, and H. J. Carmichael, Phys. Rev. Lett. **63**, 240 (1989).
5. D. Meschede, H. Walther, and G. Müller, Phys. Rev. Lett. **54**, 551 (1985).
6. G. Raithel, C. Wagner, H. Walther, L. M. Narducci, and M. O. Scully, in *Cavity Quantum Electrodynamics*, P. Berman, ed. (Academic, San Diego, Calif., 1994), and references therein.
7. K. An, J. J. Childs, R. R. Dasari, and M. S. Feld, Phys. Rev. Lett. **73**, 3375 (1994); K. An and M. S. Feld, Phys. Rev. A **52**, 1691 (1995).
8. C. Yang and K. An, Phys. Rev. A **55**, 4492 (1997).
9. H.-J. Briegel, B.-G. Englert, and M. O. Scully, Phys. Rev. A **54**, 3603 (1996).
10. M. I. Kolobov and F. Haake, Phys. Rev. A **55**, 3033 (1997).
11. P. Filipowicz, J. Javanainen, and P. Meystre, Phys. Rev. A **34**, 3077 (1986).